

Segmentation of the Common Carotid Artery with Active Shape Models from 3D Ultrasound Images

Xin Yang^a, Jiaoying Jin^b, Wanji He^b, Ming Yuchi^b, and Mingyue Ding^{b,a}

^aInstitute for Pattern Recognition and Artificial Intelligence (IPRAI), Huazhong University of Science and Technology (HUST), 1037 Luo Yu Road, Wuhan City, HuBei Province, P.R.CHINA, 430074;

^bSchool of Life Science and Technology, Huazhong University of Science and Technology (HUST), 1037 Luo Yu Road, Wuhan City, HuBei Province, P.R.CHINA, 430074

ABSTRACT

Carotid atherosclerosis is a major cause of stroke, a leading cause of death and disability. In this paper, we develop and evaluate a new segmentation method for outlining both lumen and adventitia (inner and outer walls) of common carotid artery (CCA) from three-dimensional ultrasound (3D US) images for carotid atherosclerosis diagnosis and evaluation. The data set consists of sixty-eight, $17 \times 2 \times 2$, 3D US volume data acquired from the left and right carotid arteries of seventeen patients (eight treated with 80mg atorvastatin and nine with placebo), who had carotid stenosis of 60% or more, at baseline and after three months of treatment. We investigate the use of Active Shape Models (ASMs) to segment CCA inner and outer walls after statin therapy. The proposed method was evaluated with respect to expert manually outlined boundaries as a surrogate for ground truth. For the lumen and adventitia segmentations, respectively, the algorithm yielded Dice Similarity Coefficient (DSC) of $93.6\% \pm 2.6\%$, $91.8\% \pm 3.5\%$, mean absolute distances (MAD) of $0.28 \pm 0.17mm$ and $0.34 \pm 0.19mm$, maximum absolute distances (MAXD) of $0.87 \pm 0.37mm$ and $0.74 \pm 0.49mm$. The proposed algorithm took $4.4 \pm 0.6min$ to segment a single 3D US images, compared to $11.7 \pm 1.2min$ for manual segmentation. Therefore, the method would promote the translation of carotid 3D US to clinical care for the fast, safety and economical monitoring of the atherosclerotic disease progression and regression during therapy.

Keywords: Active Shape Model (ASM), common carotid artery (CCA), atherosclerosis, three-dimensional ultrasound (3D US), carotid segmentation

1. INTRODUCTION

Based on World Health Association (WHO) statistical data, cardiovascular disease (CVDs) cause over 29% of death worldwide, a total of about 17.1 million people.¹ In the United States alone, CVD results in both direct and indirect health care costs and productivity loss amounting to \$274 billion annually.² The therapy evaluation and clinical data analysis are important to the cerebrovascular and cardiovascular pathologies diagnosis; and have attracted significant attention amongst the health and science community.^{3,4}

Ultrasound (US) has been employed as a routine examination for inexpensive non-invasive clinical diagnosis of atherosclerosis (the hardening of the arteries).^{5,6} Furthermore, three-dimensional ultrasound (3D US) imaging provides reproducible volumetric data, yielding added sensitivity to changes in plaque.^{7,8} Patients with disease of the common carotid artery (CCA) need an evaluation of the risk factors for circulation problems that can lead to blockages in the heart and brain, which can lead to morbidity and mortality.⁹ CCA inner and outer

X. Yang is with State Key Laboratory for Multi-spectral Information Processing Technologies, IPRAI, HUST, Wuhan, Hubei, China, 430074. (e-mail:xinyanghust@gmail.com). J. Jin, W. He, M. Yuchi and M. Ding are with Image Processing and Intelligence Control Key Laboratory of Education Ministry of China, Department of Biomedical Engineering, School of Life Science and Technology, HUST, Wuhan, China, 430074. (Send correspondence to M. Ding.)

Mingyue Ding: E-mail: myding@mail.hust.edu.cn, Telephone: +86-27-87792366, Address: Room 508, D11 Building, School of Life Science and Technology, East Campus, Huazhong University of Science and Technology (HUST), 1037 Luo Yu Road, Wuhan City, HuBei Province, P.R.CHINA, 430074.

contours segmentation in 3D US B-mode images is an important step in evaluating arterial disease severity and drug therapy evaluation.

Segmentation the contours of these images will also assist finding vulnerable atherosclerotic plaques susceptible to rupture causing stroke or myocardial infarction.¹⁰ Although control of the final result is given to the user during interactive segmentations, they also have errors and inconsistencies due to the variable interactions among inter-observers and intra-observers. The objective of this study is to develop and validate a segmentation method delineating the inner and outer CCA boundaries of patients with carotid stenosis and atherosclerosis. And the possible application includes: patient management, genetic research, and therapy evaluation.¹¹

Vessel contour identification in US images is still a challenge and a reoccurring problem. Currently, most physicians segment the CCA and related tissues in US images by manually tracing the boundaries to best fit the data based on their experience. Several studies were conducted to improve the quality and detection of CCA segmentations within US images.¹²⁻¹⁷

Currently, intima-media thickness (IMT) measurement of arterial thickness is the most widely used phenotype for measuring carotid atherosclerosis.¹² However, its role in clinical practice is not clear yet¹⁸ and it is difficult to repeatedly locate anatomically homologous imaging planes for longitudinal monitoring.¹⁹ A scheme for detecting the normal regions in carotid artery US images was proposed by K. B. Jayanthi *et. al.*,¹³ however, no process was taken to remove the noise in the images. CCA boundary identification pipeline, a simple and effective method, was proposed using mathematical morphology,¹⁴ but it only tested for limited lumen boundaries segmentation. L. Lou *et. al.*¹⁵ used particle motion mechanics to segment object boundaries, but it was sensitive to noise within the US images. Fast Marching Method (FMM)¹⁶ was also developed for vascular US image segmentation, extending from its original application to intravascular ultrasound (IVUS) images. A semiautomated segmentation from 3D US of carotid atherosclerosis using a level set-based method was proposed by E. Ukwatta *et. al.*,¹⁷ however, this method was a local optimum search, thus the global optimum of the parameter values can not be guaranteed.

Our purpose is therefore to develop and validate a new segmentation approach to delineate the lumen-intima boundary (LIB) and the media-adventitia boundary (MAB) of the carotid artery (CCA) from 3D US images. The key innovation of this work is based on the Active Shape Models (ASMs) segmentation for two separate time points, which used baseline data for training, and follow-up data for segmentation. And the technology enables the accurate, inexpensive, and non-invasive method for progression and regression monitoring of atherosclerosis and drug therapy evaluation.

The following of this paper is organized as follows. In Section 2, the proposed method is explained in details. The results of the scheme are shown in Section 3. Section 4 and Section 5 will contain the discussion and conclusion.

2. METHODS

In order to present the work, we firstly use ASM to segment LIB and MAB, then compare the proposed algorithm segmentation results with the manual ones. Finally, the overall performance had its validation. Figure 1 showed a sagittal cross section of a CCA with manually annotated boundaries superimposed. Figure 2 showed the manual segmentations of inner and outer walls marked on a 3D US image.

2.1 Image Acquisition

The mechanical 3D US system used in this study has been described previously in Ref.²⁰ The images were acquired by moving a linear ultrasound transducer (L12-5, Philips, Bothell, WA, USA) with an 8.5 MHz central frequency using a motorized linear device along the neck of the subject at a uniform speed of $3mm/s$ for about $4cm$ without cardiac gating.²¹

During the scanning, the video frames from the US machine were digitized, converted into a 3D US image and displayed using 3D Quantify (a multi-planar visualization software).²² 3D images were constructed from the 2D frames received from the US machine (ATL HDI 5000, Philips, Bothell, WA, USA). The voxel size in the 3D data was approximately $0.1 \times 0.1 \times 0.15 mm^3$.

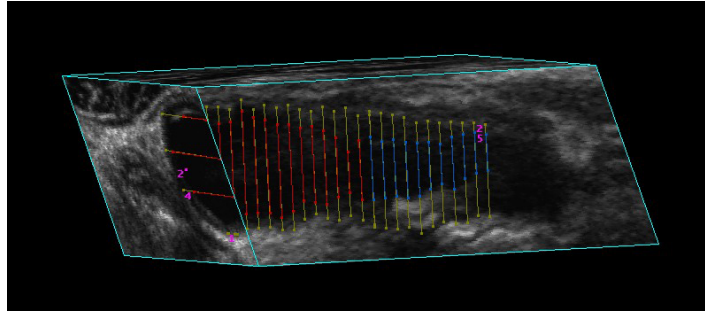


Figure 1. Sagittal cross-section of a common carotid artery (CCA) in a 3D US image. The contours on the image show the manual delineations done by the physician. The inner boundary is lumen-intima boundary (LIB) and the outer boundary is the media-adventitia boundary (MAB). The segmentations were performed on parallel inter slice distance (ISD) separated by $1mm$.

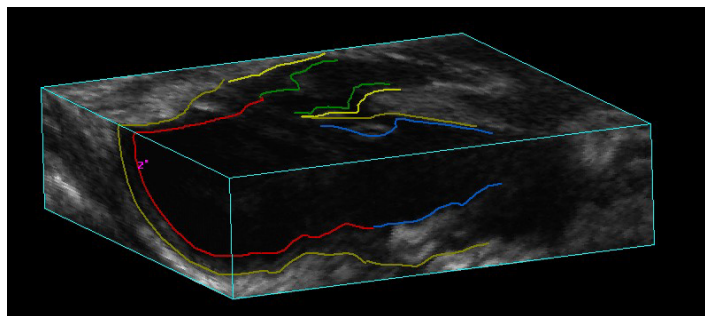


Figure 2. Long axis view of a 3D US image of carotid artery. The baseline and follow up 3D images, constructed from the set of 2D frames, were examined simultaneously to visually match the bifurcation (BF) points in both images by an operator blinded to time point and treatment. Then each 3D US image was manually segmented starting from the bifurcation point extending to 15mm into common carotid artery (CCA) and 10mm into internal carotid artery (ICA) at $1mm$ intervals perpendicular to the artery axis, as shown in Fig. 1. This study was only carried out on the CCA since the focus was on stroke risk.

The 3D Quantify ge generates 2D images of the artery by slicing through the 3D image orthogonally to the medial axis, in the inferior direction from the bifurcation (BF), with an inter slice distance (ISD) of $1mm$ (refer to Fig. 1). The expert then performed contouring of the LIB and MAB on each of these images (refer to Fig. 2).

2.2 Study Subjects

Seventeen patients with carotid stenosis over 60% were enrolled in this study (8 subjects on atorvastatin and 9 on placebo).²¹ The presence of stenosis was confirmed using carotid Doppler US flow velocities. Baseline and follow-up (3 months later) 3D US images were acquired for each subject, for both left and right carotid arteries. 8 of them, 4 males and 4 females, mean age \pm SD ($65 \pm 6.6years$), were randomly assigned to 80mg atorvastatin daily for 3 months. The remaining 9 subjects, 4 males and 5 females, mean age \pm SD ($68 \pm 8.4years$), were assigned to the placebo. All subjects, in this study, were recruited from The Premature Atherosclerosis Clinic and The Stroke Prevention Clinic at University Hospital (London Health Sciences Center, London, Canada) and the Stroke Prevention and Atherosclerosis Research Center (Robarts Research Institute, London, Canada). A written informed consent to the study protocol was provided by all of the subjects, which was approved by The University of Western Ontario Standing Board of Human Research Ethics.

2.3 Manual Segmentation

Manual segmentation of CCA boundaries is labor intensive and time-consuming.²³ There are several studies that report on semi-automated segmentation methods for delineating carotid walls on 2D US images.²⁴

The manual segmentation method used in our work was proposed by Egger *et al.*¹⁹ Prior to contouring, the expert first located the BF and defined an approximate medial axis of the carotid artery by choosing two end points of the axis. The multi-planar 3D viewing software then presented 2D images of the artery by slicing through the 3D image orthogonally to the medial axis, in the inferior direction from the BF, with an ISD of 1mm. The expert then performed contouring of arteries on each of these images. Figure 1 showed a sagittal cross-section of a common carotid artery with manually annotated boundaries overlaid. An expert outlined the vessel boundaries five times repeatedly with a single day between repetitions on transverse 2D slices extracted from 3D US images. The image sequence were randomized and the operator was blinded to the image order during each repetition to reduce memory bias.¹⁷ However, this method also still introduced the potential errors and variabilities because of the variable interactions among inter-observers and intra-observers.

2.4 Pre-processing

Several pre-processing steps were applied prior to LIB and MAB segmentation. Firstly, contrast limited adaptive histogram equalization (CLAHE)²⁵ was applied to enhance the local contrast of the US image. CLAHE partitions the image into contextual regions and applies histogram equalization by fitting a Rayleigh distribution to each region.⁸ Next, Speck Reducing Anisotropic Diffusion Method (SRAD) was used for US speckle noise reduction.²⁶ The SRAD was used to enhance the edges by inhibiting diffusion across edges and allowing diffusion on either side of the edges.

2.5 Active Shape Models (ASMs)

Active Shape Models (ASMs) are statistical models of the shape of objects, developed by Tim Cootes and Chris Taylor in 1995,²⁷ which iteratively deform to fit to an example of the object in a new image. The shapes are constrained by the point distribution model (PDM) Statistical Shape Model (SSM) to vary only in ways seen in a training set of labeled examples. The shape of an object is represented by a set of points (controlled by the shape model). The ASM algorithm aims to match the model to a new image. It works by alternating the following steps: (1) Look in the image around each point for a better position for that point; (2) Update the model parameters to best match to these new found positions. To locate a better position for each point one can look for strong edges, or a expected match to a statistical model at the point. The original methodology suggests using the Mahalanobis distance to detect a better position for each landmark point.²⁷ The technique has been widely used to analyze images of faces, mechanical assemblies and medical images (in 2D and 3D).

Following model initialization (X^o), an ASM search²⁷ is performed to segment the CCA from a new image. An ASM is defined by the equation

$$X = \bar{X} + P \cdot b, \quad (1)$$

where \bar{X} represents the mean shape, P is a matrix of the first few principal components of the shape, created by using Principal Component Analysis (PCA), and b is a vector defining the shape, whose standard deviations from the mean shape ranges between -3 and $+3$. Therefore, X is defined by the variable b . Given a set of landmark points X^i for iteration i , the goal is to find landmark points \dot{X}^i closest to the object border. The shape is then updated using Eq. (1) where

$$b = P^T \cdot (\dot{X}^i - X^i), \quad (2)$$

where each element of b can only be within ± 3 standard deviations of the mean shape. The final ASM segmentation is denoted as X^{Final} . The training of the ASM to determine \bar{X} and P is performed by manual delineation of the artery boundaries followed by manual alignment of 10 non-equally spaced landmark points (red points) along the contour (green points) as shown in Fig. 3.

It should be noted that this only needs to be performed once in an off-line setting, and once the ASM is trained it can be used for the segmentations without significant manual intervention.

Six-hundred and eighty 2D CCA images in total, extracted from the 3D US data (10 two-dimensional images per each of 17 patients of two sides at 2 time points), previously had their arterial walls manually segmented as the golden standard. Three-hundred and forty ($10 \times 17 \times 2$) 2D CCA baseline images data and manual boundaries results were used for ASM learning and training as shown in Fig. 4; while another three-hundred and forty treatment images data were used for ASM segmentation and evaluation.

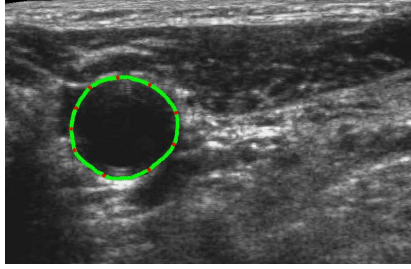


Figure 3. Ten non-equally spaced landmark points (red points) along the manual contour (green points) were randomly picked for ASM training. 340 images were labeled by senior physicians. Some of the points may be located on the weak edges.

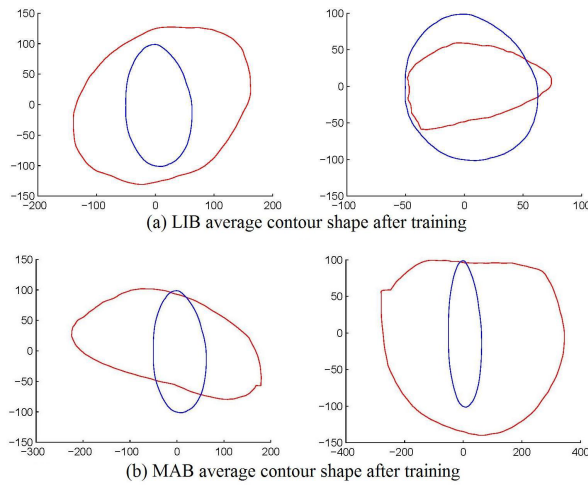


Figure 4. LIB (top) and MAB (bottom) training results of the three-hundred and forty 2D CCA baseline images data. The average shape contour would be superposed on the treatment images data as the initialization contour for ASM segmentation.

2.6 Evaluation Metrics

The Dice Similarity Coefficient (DSC) was used as a region-based measure to compare two segmentations for accuracy on slice-by-slice basis. The DSC quantifies the area overlap of two segmentations and is given by the following equation

$$DSC = 2 \frac{|R_M \cap R_P|}{|R_M| + |R_P|}, \quad (3)$$

where R_M and R_P denote the region enclosed by of the manual and proposed method boundaries, respectively.

The mean absolute distance (MAD) and maximum absolute distance (MAXD) were used as boundary distance-based metrics. And the computational time is also estimated.

3. RESULTS

Figures 5 and 6 show the segmentation results of three slices obtained using the proposed approach for a subject with a moderate level of plaque. Table 1 shows the overall evaluation results of the proposed algorithm for 340 transverse US slices extracted from 17 subjects after treatment.

3.1 Validation

The validation of new segmentation algorithm will require comparison with manual segmentation results. The accuracy, variability and reproducibility of the algorithm were evaluated by comparison to the physician-drawn

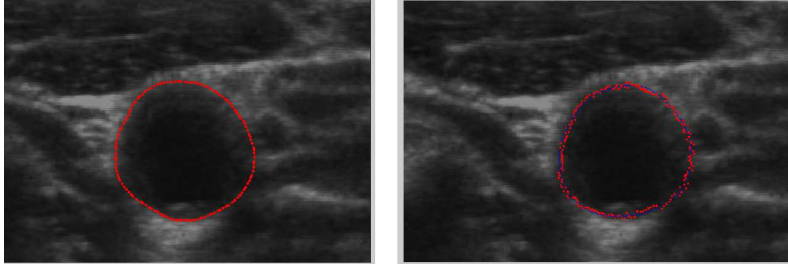


Figure 5. Adventitia results comparison after the therapy at 3 months later: original image with manual segmentation result as a golden standard (left); proposed method segmentation result (right).

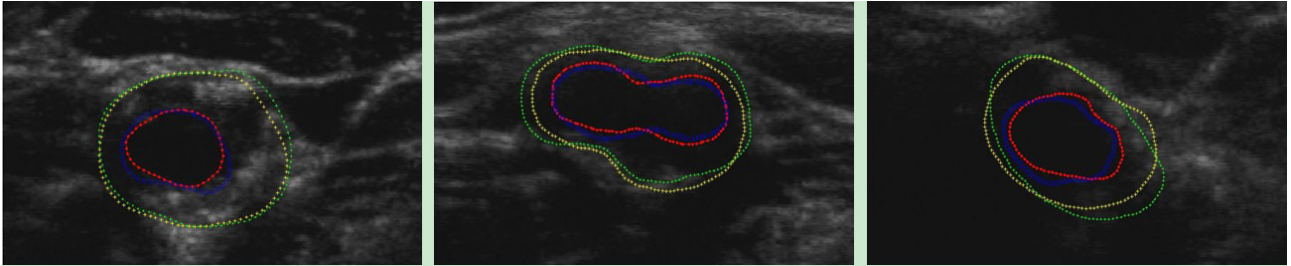


Figure 6. Sample results of the lumen and adventitia segmentations. (red/green contours: manual; blue/yellow contours: algorithm; outer contours: adventitia; inner contours: lumen.) Subject 1 (left); Subject 2 (middle) and Subject 3 (right).

contours. Three to five experts delineated the CCA boundaries on 340 2D slices. The ordering of the images was randomized to reduce learning effects. The method of Chalana and Kim²⁸ was used to compute the mean boundary from the repeated manual and algorithm-generated segmentations.

Therefore, DSC, MAD and MAXD were computed from 3D US images to obtain overall estimates of each metric for the image set. Table 1 shows the overall evaluation results of the algorithm for 340 transverse 2D US sliced images.

The proposed method yielded a DSC of $93.6\% \pm 2.6\%$ and $91.8\% \pm 3.5\%$ for the LIB and MAB, respectively. The method gave sub-millimeter error values for the MAD of $0.28 \pm 0.17mm$ and $0.34 \pm 0.19mm$, and MAXD of 0.87 ± 0.37 and 0.74 ± 0.49 for the LIB and MAB, respectively.

Our approach takes $4.4 \pm 0.6min$ compared to $11.7 \pm 1.2min$ of operator time for manual segmentation to initialize/delineate a single 3D image.⁸

4. DISCUSSION

In this paper, we presented an ASM segmentation method to delineate the LIB and MAB boundaries of the CCA from 3D US images. The algorithm yielded a higher DSC for the LIB than for the MAB, although the algorithm gave similar MAD and MAXD errors for both vascular walls. It was obvious that the lumen value is better than adventitia, which represents we got relatively better lumen segmentation result. The reasons may be: 1) different components between the two layers caused the different performance. Inside lumen is liquid blood, while the outside adventitia is complex connective tissue from the view of CCA physiology; 2) weak image edges, particularly on boundary segments that are parallel to the US beam direction is not hard for ASM learning and segmentation; 3) the initialized average contours from baseline training data have differences with the test data.

5. CONCLUSION

The main purpose of this work was to develop and evaluate a new segmentation algorithm for outlining both lumen and adventitia (inner and outer walls) of CCA from 3D US images. From a quantitative evaluation on

Table 1. Overall performance results of the proposed algorithm. Validation results of segmentation for 340 transverse slices of both left and right sides from seventeen subjects (eight with 80mg atorvastain and nine with placebo respectively) after three months treatment.

Metric	DSC (%)	MAD (mm)	MAXD (mm)
lumen-intima boundary (LIB)	93.6 ± 2.6	0.28 ± 0.17	0.87 ± 0.37
media-adventitia boundary (MAB)	91.8 ± 3.5	0.34 ± 0.19	0.74 ± 0.49

the results, we concluded that the propose method could accurately segment the CCA and also the average time saved using the algorithm was substantial.

Experimental results showed that the segmented areas could accurately define the locations of CCA contours. This method could save the physicians' time. Our work provides an easy-handle technique to simplify the job of labeling the contours in CCA manually. Therefore, the proposed method would be helpful to promote the translation of 3D carotid US to clinical care for the fast, safety and economical monitoring of the atherosclerotic disease progression and regression during therapy.

ACKNOWLEDGMENTS

This work is supported by a National Natural Science Foundation of China (NSFC) Grant No.: 30911120497/H0215 and the National 973 project Grant No.: 2011CB933103.

The authors would like to thank Dr. Aaron Fenster, Mr. Eranga Ukwatta and Dr. Wu Qiu, from Robarts Research Institute, London, Ontario, Canada, for the collaborative work on project named as "Analysis of Carotid Atherosclerosis Using 3D US Imaging".

The authors also would like to thank Dr. Xuming Zhang, Mr. Mengling Xu, Miss Kaitong Li, Miss Chuchu He, from Huazhong University of Science and Technology (HUST), for their assistance with data collection, insightful comments and revision feedback.

REFERENCES

- [1] <http://www.who.int/cardiovascular diseases/en/>, "World health organization, cardiovascular disease," (2007).
- [2] Covello, V. T. and Peters, R. G., "Women's perceptions of the risks of age-related diseases, including breast cancer: Reports from a 3-year research study," *Health Communication* **14**(3), 377–395 (2002).
- [3] Awad, J., Krasinski, A., Spence, D., Parraga, G., and Fenster, A., "Three-dimensional ultrasound-based texture analysis of the effect of atorvastatin on carotid atherosclerosis," in [*SPIE medical Imaging*], **7626**, 1–10 (2010).
- [4] Santhiyakumari, N., Rajendran, P., and et al., "Detection of the intima and media layer thickness of ultrasound common carotid artery image using efficient active contour segmentation technique," *Medical and Biological Engineering and Computing* **49**(11), 1299–1310 (2011).
- [5] Wells, P. N. T., "Current status and future technical advances of ultrasonic imaging," *Engineering in Medicine and Biology Magazine, IEEE* **19**(5), 14–20 (2000).
- [6] Lusis, A. J., "Atherosclerosis," *Nature* **407**(6801), 233–241 (2000).
- [7] Krasinski, A., Chiu, B., Spence, J. D., Fenster, A., and Parraga, G., "Three-dimensional ultrasound quantification of intensive statin treatment of carotid atherosclerosis," *Ultrasound in medicine & biology* **35**(11), 1763–1772 (2009).
- [8] Ukwatta, E., Awad, J., Ward, a. D., Samarabandu, J., Krasinski, A., Parraga, G., and Fenster, A., "Segmentation of the lumen and media-adventitia boundaries of the common carotid artery from 3d ultrasound images," in [*SPIE medical Imaging*], **7963**, 79630G–79630G–8 (2011).
- [9] Stephanian, E., "Carotid endarterectomy - a patient's guide," (<http://medinform.org/page/3948/>).

- [10] Shai, I., Spence, J. D., Schwarzfuchs, D., Henkin, Y., Parraga, G., Rudich, A., Fenster, A., Mallett, C., Liel-Cohen, N., and Tirosh, A., “Dietary intervention to reverse carotid atherosclerosis,” *Circulation* **121**(10), 1200–1208 (2010).
- [11] Spence, J. D., “Technology insight: ultrasound measurement of carotid plaquepatient management, genetic research, and therapy evaluation,” *Nature Clinical Practice Neurology* **2**(11), 611–619 (2006).
- [12] Haller, C., Schulz, J., Schmidt-Trucksass, A., Burkardt, H., Schmitz, D., Dickhuth, H. H., and Sandrock, M., “Sequential based analysis of intima-media thickness (imt) in common carotid artery studies,” *Atherosclerosis* **195**(2), e203–e209 (2007).
- [13] Balasundaram, J. K. and Banu, R. S. D. W., “A non-invasive study of alterations of the carotid artery with age using ultrasound images,” *Medical and Biological Engineering and Computing* **44**(9), 767–772 (2006).
- [14] Yang, X., Ding, M., Lou, L., Yuchi, M., Qiu, W., and Sun, Y., “Common carotid artery lumen segmentation in b-mode ultrasound transverse view images,” *International Journal of Image, Graphics and Signal Processing (IJIGSP)* **3**(5), 15–21 (2011).
- [15] Lou, L. and Ding, M., “Principle and approach of boundary extraction based on particle motion in quantum mechanics,” *Optical Engineering* **46**, 027005–027005–16 (2007).
- [16] Cardinal, M. H. R., Soulez, G., Tardif, J. C., Meunier, J., and Cloutier, G., “Fast-marching segmentation of three-dimensional intravascular ultrasound images: A pre-and post-intervention study,” *Medical physics* **37**, 3633–3647 (2010).
- [17] Ukwatta, E., Awad, J., Ward, A. D., Buchanan, D., Samarabandu, J., Parraga, G., and Fenster, A., “Three-dimensional ultrasound of carotid atherosclerosis: Semiautomated segmentation using a level set-based method,” *Medical Physics* **38**, 2479–2493 (2011).
- [18] Lorenz, M. W., Schaefer, C., Steinmetz, H., and Sitzler, M., “Is carotid intima media thickness useful for individual prediction of cardiovascular risk? ten-year results from the carotid atherosclerosis progression study (caps),” *European heart journal* **31**(16), 2041–2048 (2010).
- [19] Egger, M., Spence, J. D., Fenster, A., and Parraga, G., “Validation of 3d ultrasound vessel wall volume: an imaging phenotype of carotid atherosclerosis,” *Ultrasound in Medicine and Biology* **33**(6), 905–914 (2007).
- [20] Awad, J., Krasinski, A., Parraga, G., and Fenster, A., “Texture analysis of carotid artery atherosclerosis from three-dimensional ultrasound images,” *Medical physics* **37**, 1382–1391 (2010).
- [21] Ainsworth, C. D., Blake, C. C., Tamayo, A., Beletsky, V., Fenster, A., and Spence, J. D., “3d ultrasound measurement of change in carotid plaque volume: a tool for rapid evaluation of new therapies,” *Stroke* **36**(9), 1904–1909 (2005).
- [22] Fenster, A., Downey, D. B., and Cardinal, H. N., “Three-dimensional ultrasound imaging,” *Physics in medicine and biology* **46**, R67–R99 (2001).
- [23] Chiu, B., Egger, M., Spence, J. D., Parraga, G., and Fenster, A., “Quantification of carotid vessel wall and plaque thickness change using 3d ultrasound images,” *Medical Physics* **35**, 3691–3700 (2008).
- [24] Abolmaesumi, P., Sirouspour, M. R., and Salcudean, S. E., “Real-time extraction of carotid artery contours from ultrasound images,” 181–186, IEEE Symposium on 13th Computer-Based Medical Systems (CBMS2000) Proceedings, 2000.
- [25] Pizer, S. M., Amburn, E. P., Austin, J. D., Cromartie, R., Geselowitz, A., Greer, T., ter Haar Romeny, B., Zimmerman, J. B., and Zuiderveld, K., “Adaptive histogram equalization and its variations,” *Computer vision, graphics, and image processing* **39**(3), 355–368 (1987).
- [26] Yongjian, Y. and Acton, S. T., “Speckle reducing anisotropic diffusion,” *Image Processing, IEEE Transactions on* **11**(11), 1260–1270 (2002).
- [27] Cootes, T., Taylor, C., Cooper, D., and Graham, J., “Active shape models-their training and application,” *Computer vision and image understanding* **61**(1), 38–59 (1995).
- [28] Chalana, V. and Kim, Y., “A methodology for evaluation of boundary detection algorithms on medical images,” *Medical Imaging, IEEE Transactions on* **16**(5), 642–652 (1997).